

## Electronic Supplementary Information

### One-step electrocatalytic synthesis of ammonia and acetone from nitrogen and isopropanol in an ionic liquid

Qikun Zhang<sup>#a</sup>, Ya'nan Zhao<sup>#a</sup>, Liping Yu<sup>a</sup>, Xiaoyang Zhang<sup>a</sup>, Yiling Bei<sup>b</sup> and Bo Tang<sup>\*a</sup>

- a. College of Chemistry, Chemical Engineering and Materials Science, Key Laboratory of Molecular and Nano Probes, Ministry of Education, Collaborative Innovation Center of Functionalized Probes for Chemical Imaging in Universities of Shandong, Shandong Normal University  
Jinan 250014, P. R. China.  
E-mail: tangb@sdnu.edu.cn.

#... These authors contributed equally to this work.

- b. School of Chemistry and Chemical Engineering, Shandong University  
Jinan 250100, P. R. China.

The following equipment was used in this work: a scanning electron microscopy (SEM, SU8200, Japan), a high-resolution transmission electron microscope (HRTEM, FEI Tecnai G2 F20, USA), a Bruker AVANCE II 400 MHz nuclear magnetic resonance instrument (NMR, Bruker, Germany), a Rigaku D/Max-2400 X-ray diffractometer (XRD, Rigaku Corp., Tokyo, Japan), an ESCALAB 250 X-ray photoelectron spectrophotometer (XPS, Thermo Electron Corp., USA), a VersaSTAT 3 Princeton electrochemical workstation (Ametek-AMT, Slovakia), an alpha infrared spectrometer (IR, Bruker, Germany), an Agilent 7890A gas chromatograph (GC Agilent, USA), a UV-2600 UV-vis spectrophotometer (UV, Shimadzu Corp., Japan), a Q50 thermogravimetric analyzer (TGA, TA instruments, UK) and a DSC25 differential scanning calorimeter (DSC, TA instruments, USA).

## Characterization of the Electrode

### Scanning electron microscopy

Scanning electron microscopy (SEM) was used to analyze the surface morphology of raw and coated electrode materials. Figure S1 show the SEM images of the Fe-modified SSM.

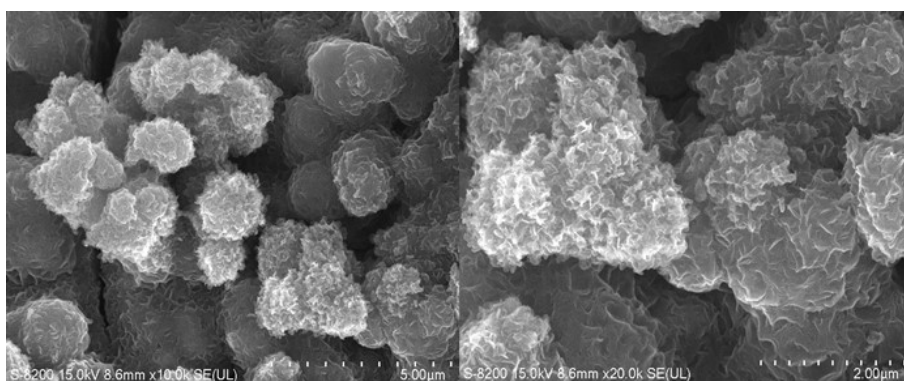


Figure S1. SEM images of a Fe-modified SSM.

### High resolution transmission electron microscopy

In this paper, high resolution transmission electron microscopy (HRTEM) was used to characterize the species morphology and lattice of the the two prepared working electrodes. Figure S2 show the HRTEM images of a Fe-modified SSM.

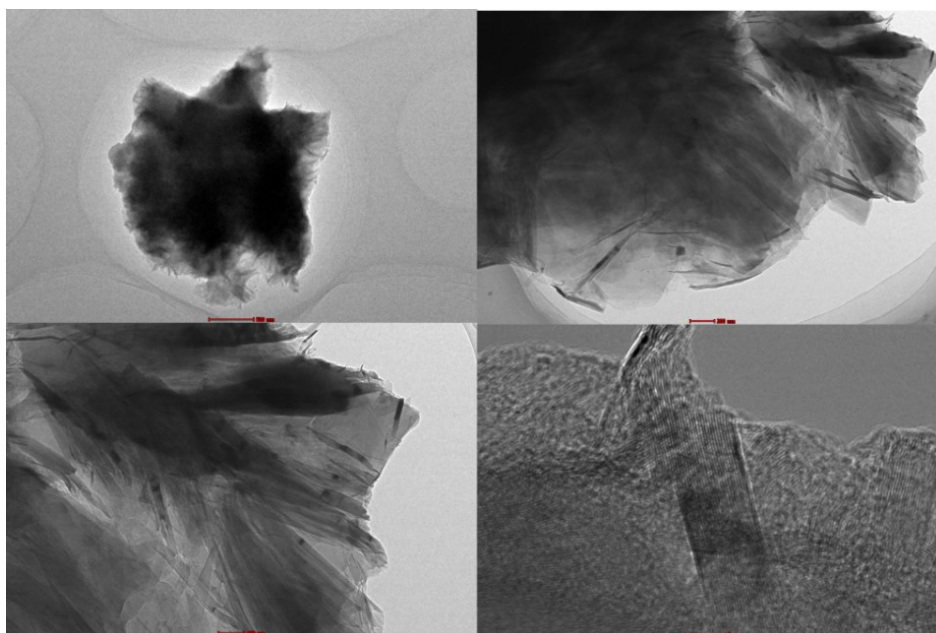
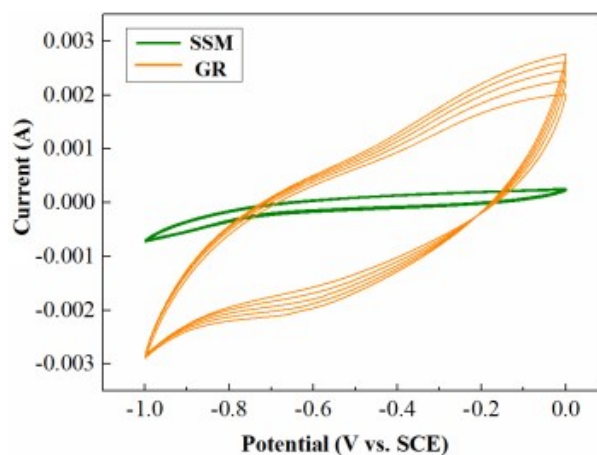


Figure S2. HRTEM images of a Fe-modified SSM.

## Cyclic voltammetry

The working electrode was prepared by cyclic voltammetry (CV) in a standard three-electrode system. A saturated calomel electrode (SCE) was used as the reference electrode, the auxiliary electrode was a platinum electrode, and the working electrode was a Fe-modified GR and Fe-modified SSM.



**Figure S3.** CV curves of electrodeposition in 0.1 M FeSO<sub>4</sub> (voltage range, -1~0 V; scanning rate, 20 mV/s).

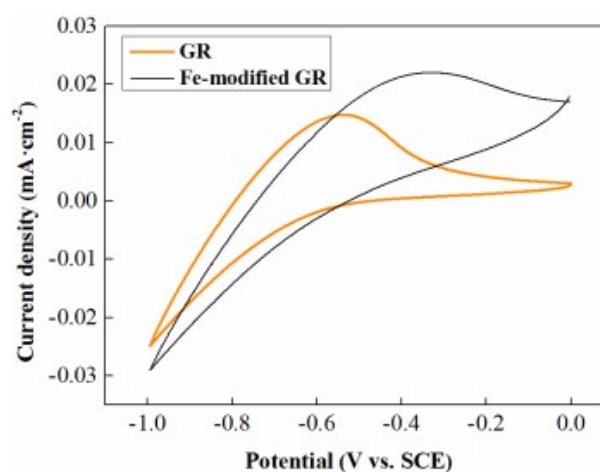


**Figure S4.** CV curves of GR and Fe-modified GR in 0.1 M KOH (voltage range, -1~0 V; scanning rate, 20 mV/s)

The double-layer capacitance ( $C_{DL}$ ) was determined by CV (Figure S5). The  $C_{DL}$  values of the pure GR and the Fe-modified GR were 0.43 mF·cm<sup>-2</sup> and 1.23 mF·cm<sup>-2</sup>, respectively. The roughness factor (RF) of the Fe-modified GR was approximately 12, which indicated that the material was suitable for the electrochemical synthesis of ammonia.

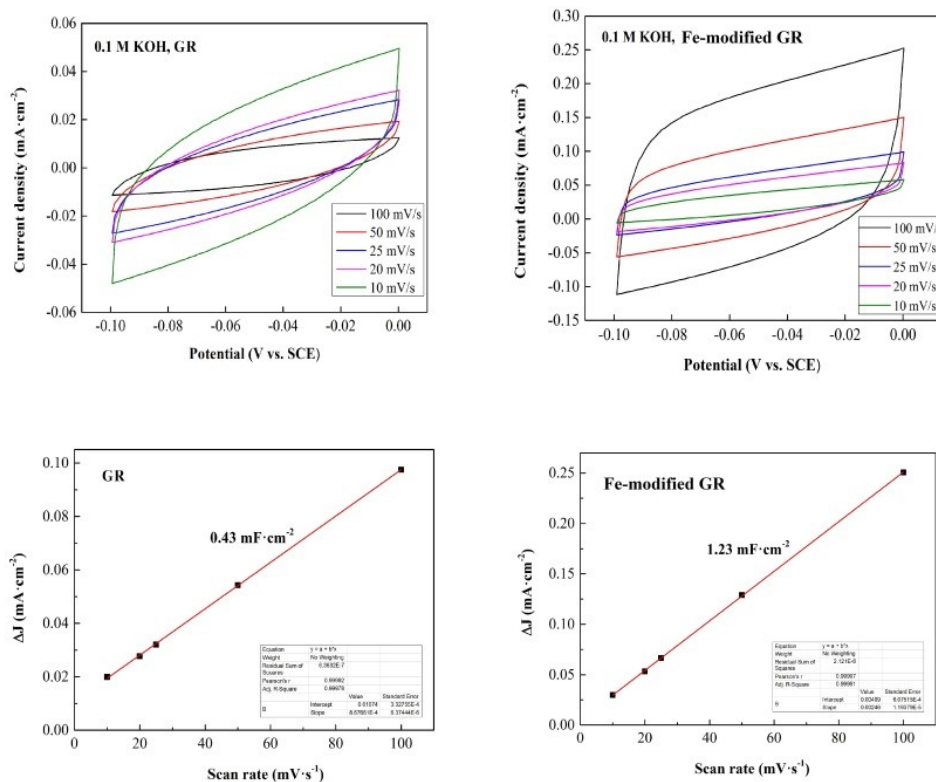


**Figure S5.** CV curves of GR and Fe-modified GR. a) CV curves of the GR electrode at different scanning rates; b) CV curves of the Fe-modified GR at different scanning rates; c) relationship between the scanning current density difference of the GR before and after 0.05 V vs scanning rate; d) relationship between scanning current density difference of Fe-modified GR before and after 0.05 V vs scanning rate.

## Linear sweep voltammetry

In this paper, linear sweep voltammetry (LSV) was used to measure the nitrogen reduction activity. The LSV of the ionic liquid electrolyte saturated with N<sub>2</sub> or Ar was tested under the following conditions: a voltage of 0 to -1 V (vs. SCE) and a scanning rate of 20 mV/s. From -0.6 V to -1 V, the current density in the N<sub>2</sub> atmosphere was slightly higher than that in the Ar atmosphere (Figure S6).

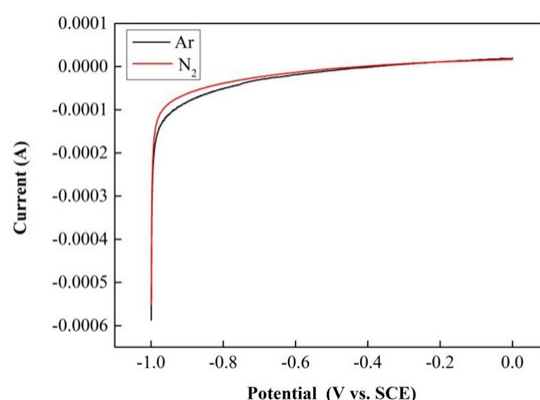


**Figure S6.** LSV curves in a N<sub>2</sub> or Ar atmosphere.



## Conductivity of [P<sub>6,6,6,14</sub>] [F<sub>6</sub>P]

Good conductivity is necessary for the realization of the electrochemical ammonia synthesis process. As shown in Fig. S9, with increasing concentration, the conductivity of the ionic liquid also increased and was higher than that of water ( $1.0 \times 10^{-3}$  S/M), indicating that the ionic liquid was existed in the form of ions at the measured temperature.

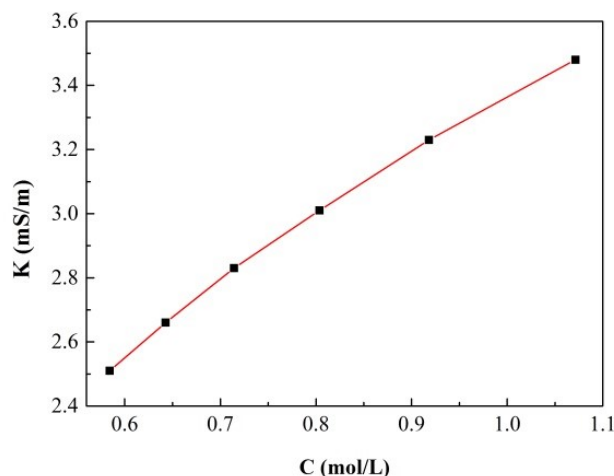


Figure S9. Conductivity of the ionic liquid [P<sub>6,6,6,14</sub>] [F<sub>6</sub>P].

## Thermal stability analysis

The thermal stability was measured by a Q50 thermogravimetric analyzer in the temperature range of 25-550 °C under a N<sub>2</sub> atmosphere (30 ml/min) at a heating rate of 10 °C/min. As shown in Figure. S10, the first weight loss of the ionic liquid occurred at 350 °C, and the maximum thermal decomposition temperature was approximately 400 °C, indicating that [P<sub>6,6,6,14</sub>][F<sub>6</sub>P] has high thermal stability.

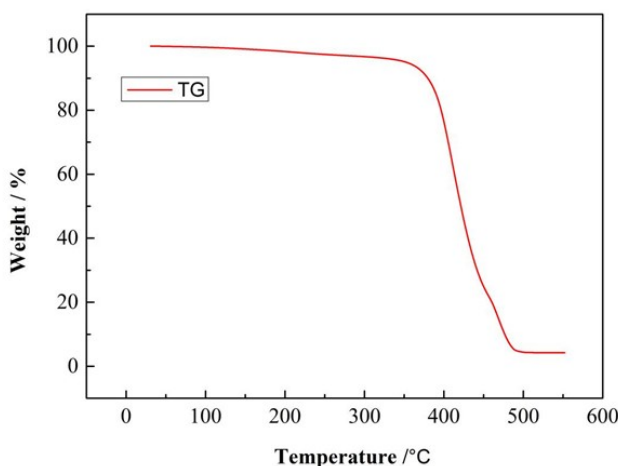
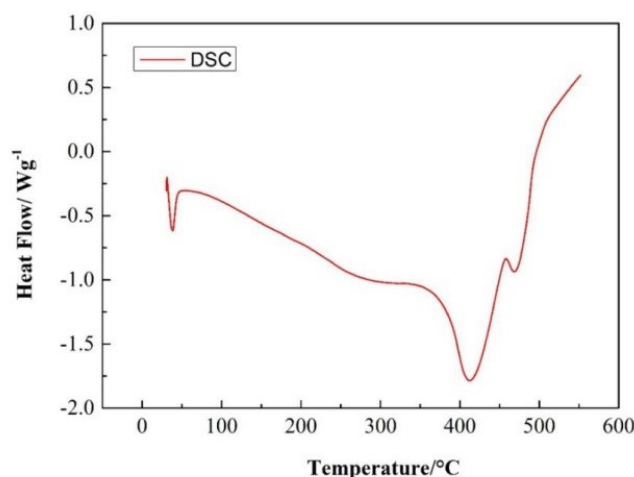


Figure S10. TG curve of the ionic liquid [P<sub>6,6,6,14</sub>][F<sub>6</sub>P]

## Calorimetric analysis

The thermal transformation performance of ionic liquids was tested by a DSC25 differential scanning calorimeter at a heating rate of 10 °C/min in the range of 25-550 °C under a N<sub>2</sub> atmosphere (30 ml/min). As shown in Figure S11, the melting point of the ionic liquid was 38.5 °C, and decomposition occurred at 412.8 °C. However, no crystallization or melting endothermic peaks were observed on the DSC curves of [P<sub>6,6,6,14</sub>][F<sub>6</sub>P], indicating that the degree of crystallization of the ionic liquids was relatively low.



**Figure S11.** DSC curve of the ionic liquid [P<sub>6,6,6,14</sub>][F<sub>6</sub>P].

### Solubility of [P<sub>6,6,6,14</sub>][F<sub>6</sub>P]

The characteristics of ionic liquids differ from those of molecular solvents, and such liquids have great polarity. Therefore, it is of considerable significance to study the solubility of ionic liquids in organic solvents. The solubility of ionic liquids in organic solvents is closely related to the anions and cations present. One milliliter of [P<sub>6,6,6,14</sub>][F<sub>6</sub>P] and 1 ml of different organic solvents were added to a colorimetric tube with a stopper, and the results are shown in Table S1.

### Purity analysis of [P<sub>6,6,6,14</sub>][F<sub>6</sub>P]

The ionic liquid [P<sub>6,6,6,14</sub>][F<sub>6</sub>P] was synthesized by a replacement reaction of trihexyltetradecalphosphoride (C<sub>32</sub>H<sub>58</sub>BrP) and ammonium hexafluorophosphate (NH<sub>4</sub>PF<sub>6</sub>) in acetone. The reaction conditions were mild, and no byproducts were produced. After NH<sub>4</sub>Br was separated by vacuum filtration, the final ionic liquid may contain unreacted Br<sup>-</sup>. We used the 1 mol/L AgNO<sub>3</sub> solution to test whether there was light yellow flocculent precipitation (AgBr) in the last washing solution. Finally, the absolute ionic liquid product was obtained.

### Yield and density calculations of [P<sub>6,6,6,14</sub>][F<sub>6</sub>P]

After NH<sub>4</sub>Br and Br<sup>-</sup> were separated, the prepared ionic liquid was dried in a vacuum drying oven for 48 hours to a constant weight. The yield and product density were calculated according to the following formulas.

$$Y = \frac{n_{C_{32}H_{58}PBr}}{n_{C_{32}H_{58}PBr}} \times 100\% \quad \text{Eq. 1}$$

$$\text{Amount of substance: } n = \frac{m}{M} \quad \text{Eq. 2}$$

According to Eq. 1 and 2, the yield of the ionic liquid was 78%.

$$\text{Density: } \rho = \frac{m}{V} \quad \text{Eq. 3}$$

According to Eq. 3, the density of the ionic liquid was 1.1507 g/ml.

## Electrocatalytic synthesis of ammonia

The electrochemical ammonia synthesis at ambient temperature and atmospheric pressure was realized by CV. The working electrodes were GR and a SSM freshly deposited with nano-Fe. A Pt electrode was used as the auxiliary electrode, and a saturated calomel electrode was used as the reference electrode. The current density of ammonia synthesis with a Fe-modified GR as the working electrode was higher than that with a Fe-modified SSM electrode (Figures S13-S14).



**Figure S12.** Experimental apparatus of the electrochemical reduction of  $N_2$  to  $NH_3$ .

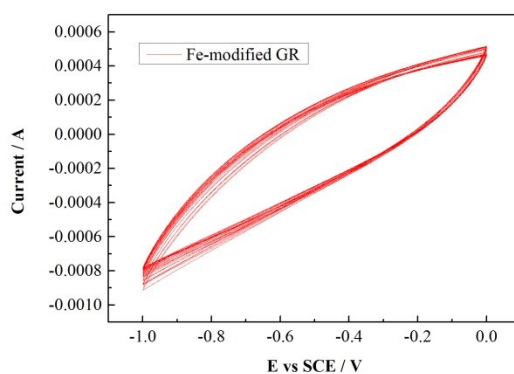


**Figure S13.** CV curves for ammonia synthesis by electrochemical reduction of nitrogen with a Fe-modified GR. (electrolyte 50.00 mL, scanning voltage rate  $20 \text{ mV}\cdot\text{s}^{-1}$ , voltage range  $-1.0 \text{ V}\sim 0.0 \text{ V}$ , 30 cycles).

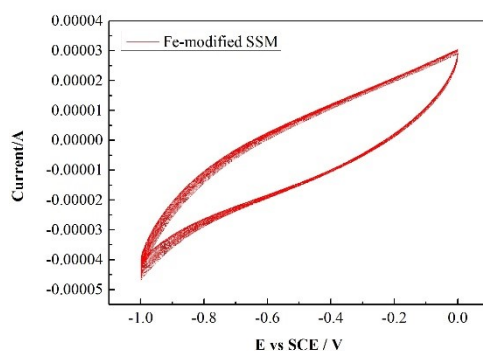


**Figure S14.** CV curves for ammonia synthesis by electrochemical reduction of nitrogen with Fe-modified SSM. (electrolyte 50.00 mL, scanning voltage rate  $20 \text{ mV}\cdot\text{s}^{-1}$ , voltage range  $-1.0 \text{ V}\sim 0.0 \text{ V}$ , 30 cycles).

## Ammonia Detection

In this study, the  $\text{NH}_3$  yield by electrocatalytic nitrogen reduction was determined by the indophenol blue method. After being absorbed by the absorption solution (0.005 M  $\text{H}_2\text{SO}_4$ ), ammonia reacted with salicylic acid to form a blue-green indophenol blue dye in the presence of sodium nitroprusside and sodium hypochlorite.

The standard curve was plotted as follows. First, preparing a series of reference solutions, by pipetting suitable volumes of the  $\text{NH}_4\text{Cl}$  working solution in colorimetric tubes; Second, making up to the mark with 0.005 M  $\text{H}_2\text{SO}_4$  aqueous solution to 10 mL; Third, adding 0.1 mL of 1% sodium nitroprusside solution, 0.1 mL of 0.05 M sodium hypochlorite and 0.5 mL of 5% salicylic acid solution to each of the tubes and mix thoroughly, allowing above solutions to sit for 1h for color development. Water was the blank, and the absorbance of each tube solution was measured by a spectrophotometer at 697.5 nm in a 1.0 cm cuvette. Please refer to ref. 1 for specific preparation of standard solutions.

Taking the ammonia concentration ( $\text{mg}\cdot\text{L}^{-1}$ ) as the abscissa and the absorbance as the ordinate, a standard curve was drawn. The linear equation of the regression line and the correlation coefficient of the standard curve were calculated. According to the same procedure of drawing the standard curve, 1.0 mL of sample was added to a colorimetric tube and reacted with chromogenic substrates. The absorbance of the sample was determined. The concentration of ammonia in the sample was calculated according to the linear equation of the standard working curve, and the yield of electrocatalytic ammonia synthesis was calculated eventually.

The standard curve equation was  $Y=0.87896X+0.03538$ , the linear correlation coefficient was  $R^2=0.9998$ , and the minimum detection concentration was  $0.05\ \mu\text{g}\cdot\text{mL}^{-1}$  (Figure S15).

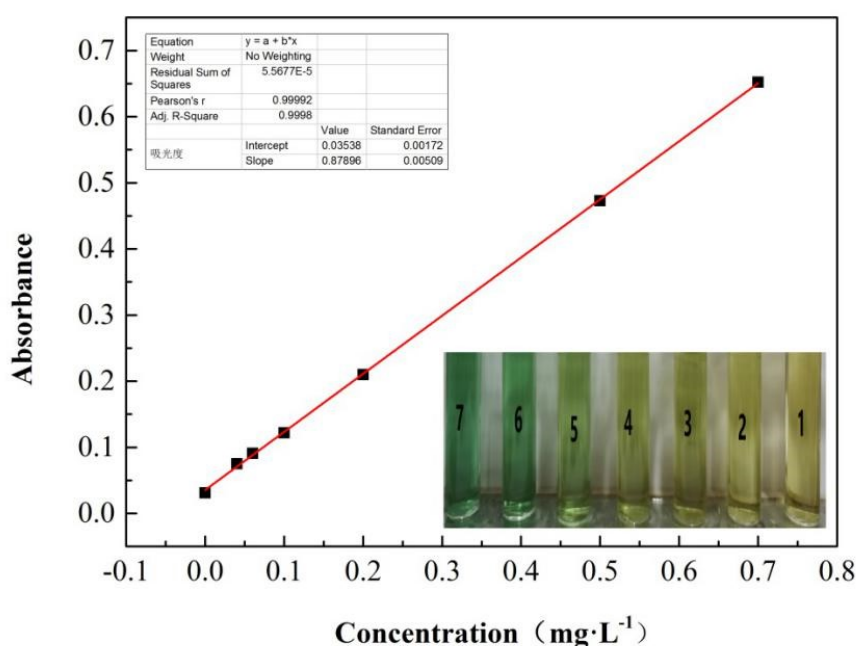


Figure S15. Standard curve for ammonia detection.

## Acetone determination

In this study, we used GC analysis of the mixture to determine the acetone yield. An Agilent 7890A gas chromatograph with a quartz capillary column was used. The stationary phase was 6% cyanopropylbenzene and 94% dimethylsiloxane. The analysis conditions for gas chromatography were as follows: The column temperature and inlet temperature were 200 °C; the flow of carrier gas nitrogen was  $5.0\ \text{mL}\cdot\text{min}^{-1}$ , and the split ratio was 3:1; the detector was a flame ionization detector with hydrogen flame ionization at 280 °C; the  $\text{H}_2$  flow rate was  $30\ \text{mL}\cdot\text{min}^{-1}$ ; the air flow rate was  $300\ \text{mL}\cdot\text{min}^{-1}$ ; and the sample injection volume was  $1.0\ \mu\text{L}$ . The contents of acetone in the absorption solution, the washing bottle and isopropanol were detected, respectively.

## Supplementary Tables

**Table S1.** Dissolution of ionic liquids in some solvents

Number	Solvent	Ionic liquid [P <sub>6,6,6,14</sub> ][F <sub>6</sub> P]
1	methanol	soluble
2	ethanol	soluble
3	ethylene glycol	insoluble
4	dichloromethane	soluble
5	acetone	soluble
6	benzene	soluble
7	anhydrous diethyl ether	soluble
8	formaldehyde	insoluble
9	2-butoxy ethanol	soluble
10	acetonitrile	soluble
11	<i>N,N</i> -dimethylformamide	soluble
12	aniline	soluble
13	benzyl Ether	soluble
14	carbon tetrachloride	soluble
15	benzyl chloride	soluble
16	chloroform-d	soluble
17	isopropanol	soluble
18	water	insoluble

**Table S2.** Experimental values of N<sub>2</sub> solubility in prepared ionic liquids at 30°C, adjusted to a partial pressure of 101325 Pa, expressed as mole fraction ( $\chi_2$ ), molar concentration  $c_{N_2}$ , and molar concentration  $b_{N_2}$ .  $P_{eq}$  is the experimental equilibrium pressure and  $\rho$  is the density at which N<sub>2</sub> solubility was calculated.

Item	[P <sub>6,6,6,14</sub> ][F <sub>6</sub> P]	[P <sub>6,6,6,14</sub> ][eFAP] <sup>[a]</sup>	H <sub>2</sub> O <sup>[b]</sup>
$P_{eq}/10^4\text{Pa}$	9.98	9.64	9.88
$\rho/\text{g} \cdot \text{cm}^{-3}$	1.1507	1.1991	1.000
$\chi_2/10^{-3}\pm 2\%$	4.5	3.2	0.01
$C_{N_2}/\text{mmol} \cdot \text{L}^{-1}\pm 2\%$	5.8	4.1	0.58
$b_{N_2}/\text{mmol} \cdot \text{kg}^{-1}\pm 2\%$	5.2	3.5	0.58

[a] The data are from reference 2; [b] the data are from reference 3.

**Table S3.** Absolute energy and relative energy of species calculated at the B3LYP/6-311G\*\* level

Item	Energy / a.u.
N <sub>2</sub>	-109.4710
C <sub>3</sub> OH	-194.2986
C <sub>3</sub> OH-N <sub>2</sub>	-303.7740
[P <sub>6,6,6,14</sub> ][F <sub>6</sub> P]	-2541.7870
[P <sub>6,6,6,14</sub> ][F <sub>6</sub> P]-N <sub>2</sub>	-2651.2607
H <sub>2</sub> O	-76.3861
H <sub>2</sub> O-N <sub>2</sub>	-185.8592

$$\Delta E_1 = E_{C_3-OH-N_2} - E_{C_3-OH} - E_{N_2} = -0.0044 \text{ a.u.} = -11.6 \text{ kJ/mol}$$

$$\Delta E_2 = E_{P-F-N_2} - E_{P-F} - E_{N_2} = -0.0027 \text{ a.u.} = -7.09 \text{ kJ/mol}$$

$$\Delta E_3 = E_{H_2O-N_2} - E_{H_2O} - E_{N_2} = -0.0021 \text{ a.u.} = -5.51 \text{ kJ/mol}$$

## References

- [1] Q. Zhang, B. Liu, L. Yu, Y. Bei, B. Tang, *ChemCatChem* **2020**, *12*, 334-341
- [2] C. S. M. Kang, X. Zhang and D. R. MacFarlane, *J. Phys. Chem. C*, 2018, **122**, 24550-24558.
- [3] S. Mao and Z. Duan, *Fluid Phase Equilib.*, 2006, **248**, 103-114.